RSC Advances

RSC Publishing

PAPER

View Article Online
View Journal | View Issue

Dextrin cross linked with poly(HEMA): a novel hydrogel for colon specific delivery of ornidazole†

Cite this: *RSC Adv.*, 2013, **3**, 25340

Dipankar Das,[a] Raghunath Das,[a] Paulomi Ghosh,[b] Santanu Dhara,[b] Asit Baran Panda[c] and Sagar Pal*[a]

We report on the synthesis and characterization of a novel hydrogel based on dextrin grafted with poly(2-hydroxyethyl methacrylate) by embedding *N*,*N*′-methylene bis acrylamide (MBA) as cross linker, into a polymeric network in the presence of potassium persulphate (KPS) initiator for colon specific delivery of ornidazole. Various grades of hydrogels [Dxt-g-p(HEMA)] have been synthesized by altering the reaction parameters and the best one optimized. The developed hydrogel has been characterized using FTIR spectra, ^{13}C NMR spectra, elemental analysis, XRD study, SEM analysis, TGA analysis, swelling study and cell viability study. The equilibrium swelling ratio of the hydrogels has been recorded in different media and found to be at a maximum at pH 7.4. A cell viability study indicates that the hydrogel is non-cytotoxic in nature. The drug delivery results demonstrate that Dxt-g-p(HEMA) delivers ornidazole successfully in the colonic region in a controlled way and is a good candidate for an orally administered drug delivery system. The release mechanism and kinetics of ornidazole from various hydrogels have been determined using different linear and nonlinear mathematical models, which confirm that ornidazole release from hydrogel follows first order kinetics and a non-Fickian diffusion mechanism.

Received 28th August 2013
Accepted 17th September 2013

DOI: 10.1039/c3ra44716b

www.rsc.org/advances

1. Introduction

In recent years, hydrogels have drawn significant attention because of their numerous applications in the pharmaceutical and biomedical fields.[1] Hydrogels are physically or chemically cross linked natural or synthetic three dimensional polymer networks, which are capable of absorbing large amounts of water while maintaining their structure. Remarkable attempts have been made to design and develop novel hydrogels with combined characteristics like, tuneable chemical and three-dimensional physical structure,[2] desired mechanical properties,[3] high water content capability and biocompatibility,[2] all of which are essential for applications in tissue engineering, biomedical implants, drug delivery, and nano-biotechnology.[4]

More recently, natural polymer-based hydrogels have attracted ample interest in tissue engineering and drug delivery applications.[5] They can be obtained with various desired properties similar to their synthetic counter-parts and hence hydrogels are employed alone or with their modified forms in pharmaceutical and biomedical fields as they are biodegradable, abundant in nature, renewable, non-toxic, and relatively cheap. However, natural polymers have certain drawbacks, like uncontrolled rate of hydration, microbial contamination, and drop in viscosity on storing. Fortunately, several strategies have already been developed to overcome these drawbacks by suitable chemical modification. One of the most significant ways to modify natural polymers is grafting of synthetic polymers onto their backbones. The insoluble nature of grafted hydrogels is mainly because of the chemical and/or physical cross links. It is also easy to tune the physico-chemical properties of grafted hydrogels, which are sensitive towards various stimuli present in our body like pH, ionic strength, temperature *etc.*, owing to flexible synthetic methods.[6] Thus, use of these graft copolymer based hydrogels, specifically for drug delivery applications is advantageous over other developed biomaterials based on hydroxyapatite, collagen, chitosan, alginate and nano-composites,[7] as the drug release behaviour of these hydrogels not only depends on the extent of cross linking but also on various other factors, including swelling properties, pH of the release media and finally for their biocompatibility. In particular, for colon specific drug delivery, pH-sensitive hydrogels have attracted increasing attention in a stimuli-responsive manner based on pH changes in GI tract. In recent years, several natural polymer based hydrogels have been reported for colon specific delivery, but their release characteristics as well as drug stability are not satisfactory from a pharmacological point of view.[8]

[a]*Polymer Chemistry Laboratory, Department of Applied Chemistry, Indian School of Mines, Dhanbad-826004, India. E-mail: sagarpal1@hotmail.com; Fax: +91-326-2296615; Tel: +91-326-2235769*

[b]*School of Medical Science & Technology, Indian Institute of Technology, Kharagpur – 721302, India*

[c]*Discipline of Inorganic Materials and Catalysis, Central salt and Marine Chemicals Research Institute (CSIR), Bhavnagar-364002, Gujarat, India*

† Electronic supplementary information (ESI) available: Table containing drug release kinetics parameters, stability study result. See DOI: 10.1039/c3ra44716b

Further, several antibiotics, such as ciprofloxacin,[9] metronidazole,[10] ornidazole,[8a] tetracycline hydrochloride[11] have been used for treatment of colon related disorders. Out of these ornidazole is the preferred drug, mostly used in the treatment of severe hepatic and intestinal amoebiasis, as it has antiprotozoal and antibacterial properties against anaerobic bacteria.[8a,11,12] It is used in the treatment and prophylaxis of susceptible anaerobic infections in gastric surgery.[12] However, due to the complete and prompt absorption after oral administration and short biological half life of ornidazole,[8a] it is essential to deliver the drug in a more sustained way to provide longer bioavailability and hence its administration in tablet form may provide a minimum amount of ornidazole for local action in the colon.[8a] In spite of the development of various drug delivery systems, like carboxymethyl chitosan hydrogel, hydrogel based on sterculia gum–polyHEMA–polyacrylic acid, hydrogel derived from sterculia gum and poly(vinyl pyrrolidone), HPMC, and ethyl cellulose, to investigate the colon specific release behaviour of ornidazole, it is essential to develop new colon specific delivery systems for ornidazole to overcome important shortcomings of developed hydrogels, like specificity, biodegradability, biocompatibility, drug stability, and most importantly controlled release properties.[8a–d] For example, Singh *et al.*[8b] reported that ~65% of ornidazole drug was released from sterculia-*cl*-poly(HEMA-*co*-AAc) hydrogel in 5 h, Vaghani *et al.*[8a] reported ~100% ornidazole release in 12 h from the carboxymethyl chitosan hydrogel system. Singh *et al.*[8d] also reported the controlled release behaviour of ornidazole from sterculia-*cl*-poly(NVP) hydrogel. Further, the non-cytotoxicity of the materials and the stability of the drug in that matrix are also the vital factors for a material to be a novel and useful drug delivery system. Unfortunately, based on our knowledge, there are no literature reports on the toxicity level as well as the ornidazole stability in these matrices, except that Patel *et al.*[8c] studied the ornidazole release from HPMC based coated system, which released the drug ~65% in 12 h and the stability of drug loaded tablet after 2 months for 12 h is ~74–78% and for 24 h is ~96–98% at 40 ± 2 °C/75 ± 5% RH. In view of the potential pharmaceutical importance of ornidazole and the lack of literature on the non-cytotoxic and compatible matrix for oral administration of ornidazole in a sustainable way through prolonged control release, it is essential to develop a novel natural polymer based hydrogel, which is non-toxic, compatible with the drug and shows a more controlled/sustained ornidazole release behaviour.

Out of various natural polymers, pure/modified polysaccharide-based hydrogels are the most interesting and the most used because of their high content of functional groups, like hydroxyl, amino, carboxylic acid groups, which are utilized for cross linking with additional functional cross linkers as well as further bioconjugation with cell targeting agents.[13] In recent years, polysaccharide based graft copolymer hydrogels have been a new entrance in the field of controlled drug delivery by solving the shortcomings as mentioned above for natural polymers.[14] Dextrin, one of the most promising natural polysaccharides, is enzymatically degradable and hydrophilic in nature. It is water soluble, optically active, low viscosity, non-toxic and an ideal polymer to form hydrogels. Previously, it has been reported that various synthetic polymers such as polymethyl acrylate, polyvinyl acrylate, polyacrylamide and so on have been introduced on the dextrin backbone for their application in different fields.[15] It has also been reported that cross linking density is very crucial for desirable polymeric network formation and its application in the biomedical field.[16] On the other hand, poly-2-hydroxy ethyl methacrylate [poly(HEMA)] based hydrogels recently received great attention in biomedical applications, such as corneal implants, cardiovascular implants, contact lenses, tissue repair surgery, dental applications as well as in the controlled release of antibiotic drugs, anti cancer drugs, peptides, proteins.[17] HEMA can be polymerized either by the homo-polymerization or copolymerization technique.[18] Because of its biocompatibility, poly(HEMA) can act as an ideal component for various biomedical and pharmaceutical applications. Although, HEMA–different polysaccharide based hydrogels have already been developed for other purposes, to the best of our knowledge there is no report on a hydrogel based on poly(HEMA) and dextrin *i.e.* Dxt-g-p(HEMA). Thus, it is presumed that the grafted hydrogel derived from dextrin and poly(HEMA) may be a probable potential candidate for colon specific drug delivery of ornidazole.

Considering all these assertions and in order to improve the effectiveness of dextrin as a recipient for a colon specific drug delivery system, poly(HEMA) has been grafted on the dextrin backbone in the presence of *N*,*N*′-methylene bis acrylamide (MBA) as a cross linker. The developed hydrogel showed excellent pH dependent swelling behaviour, which favours its applicability as a colon targeted drug delivery agent. Further, the developed hydrogel is non-cytotoxic, released the enclosed ornidazole drug in a more sustained way and most importantly the drug loaded tablet is stable (~98%) up to 3 months. To the best of our knowledge, this is the first investigation on the preparation of a dextrin and poly(HEMA) based hydrogel and on its use as carrier for colon specific ornidazole delivery.

2. Experimental

2.1 Chemicals

Dextrin was purchased from Fluka, Switzerland. 2-Hydroxyethyl methacrylate (HEMA) was procured from Alfa Aesar, Lancaster, UK. *N*,*N*′-Methylene bis acrylamide (MBA) was acquired from Loba Chemie Pvt. Ltd., Mumbai, India. Potassium persulphate (KPS) was supplied by Glaxo Smith Kline Pharmaceuticals Ltd., Mumbai, India. Acetone was obtained from E-Mark (I) Pvt. Ltd., Mumbai, India. Ornidazole was a gift sample from Endoc Pharma, Rajkot, Gujarat, India. Polyvinyl pyrrolidone (PVP-K30) was supplied by Spectrochem Pvt. Ltd., Mumbai, India. Double distilled water was used in all experimental works.

2.2 Synthesis

Preparation of hydrogel. The network hydrogel based on dextrin grafted with poly(HEMA) in the presence of MBA cross linker was prepared by a free radical polymerization technique.

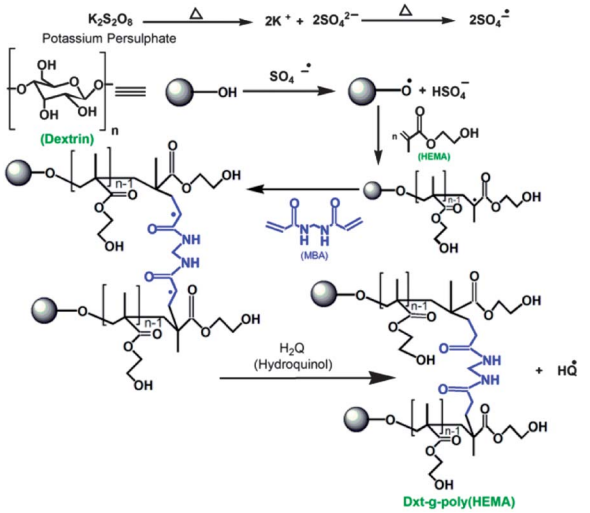

Scheme 1 Schematic representation of the synthesis of Dxt-g-p(HEMA) hydrogel.

A typical experimental procedure for the co-polymerization reaction is as follows and summarised in Scheme 1: 1 g of dextrin was slowly dissolved in 80 mL of distilled water in a three necked round bottom flask. The flask was fitted with an electrically operated magnetic stirrer (Tarsons, Model: Spinot Digital) and kept in an oil bath maintained at a temperature of 50 °C, with constant stirring (having a stirring speed of 400 rpm). Thereafter, an aqueous solution of initiator (*i.e.* KPS) followed by monomer *i.e.* HEMA was added one after another in the dextrin solution and the temperature of the reaction mixture was increased up to 80 °C. Then, the required amount of cross linker (*i.e.* MBA) given in Table 1 was introduced in the reaction mixture having the same temperature and stirring speed. During the whole reaction, nitrogen gas was purged through the reaction system. The graft copolymerization reaction was allowed to proceed at 80 °C for 3 h, followed by termination of the reaction using a saturated solution of hydroquinol. The resultant reaction mixture (*i.e.* mixture of hydrogel and homopolymer, if so formed) was cooled to room temperature, dispersed in acetone, so that the homopolymer [*i.e.* poly(HEMA)] and excess MBA will go into solution. The precipitate was pure hydrogel, free from any homopolymer. Finally the hydrogel was collected, and dried in a vacuum oven at 40 °C, until and unless constant weight was accomplished. The synthesis details are represented in Table 1.

2.3 Characterization

FTIR spectra of the dextrin, Dxt-g-p(HEMA) 5 hydrogel, ornidazole drug and the triturated form of the tablet were recorded using the KBr pellet method (Model IR-Perkin Elmer, Spectrum 2000). The scan range was 400 and 4000 cm^{-1}.

C, H, N analysis was performed using an Elemental Analyzer (Vario EL III, Elementar, Germany). The C, H, N analysis was carried out by the combustion process. In this procedure, the sample was burned in presence of excess oxygen, and various traps collect the combustion products: carbon dioxide, water, and nitric oxide. The masses of these combustion products can be used to calculate the composition of the unknown sample.

Solid state ^{13}C nuclear magnetic resonance (NMR) spectra of dextrin and the hydrogel were recorded at 500 MHz on a Bruker Advance II-500NMR spectrophotometer.

Wide angle X-ray diffraction (XRD) behaviour of the hydrogel, ornidazole drug and triturated form of tablet were recorded using a Bruker X-ray diffractometer (Bruker, D8-Fecus, Germany).

The surface morphologies of neat dextrin and the hydrogel were investigated using scanning electron microscopy. After complete drying, the polysaccharide and the hydrogel were sputter-coated with gold, and the surface morphologies were analyzed by SEM (Model: S-3400N, HITACHI, Japan).

Thermogravimetric analysis of the native dextrin and the hydrogel was carried out with a TGA analyzer (Model – DTG 60, Shimadzu, Japan) in the presence of an inert atmosphere of nitrogen. The heating rate was uniform in both cases *i.e.* 5 °C min^{-1}.

2.4 Measurements of equilibrium swelling capacity and swelling kinetics

The equilibrium swelling ratio (ESR) of hydrogels was assessed in pH 1.2, 6.8 and 7.4 at 37 °C. A known amount (0.5 g) of dried hydrogel was immersed in buffer and then left to swell for 10 h. The swollen hydrogel was withdrawn after every 1 h and the excess water was blotted off carefully using tissue paper and

Table 1 Synthesis details and equilibrium swelling characteristics of various hydrogels

	Amount of dextrin = 0.0062 mol (*i.e.* 1 g) for all hydrogel syntheses						
					Equilibrium swelling (%)		
Hydrogel	Initiator conc. (mole × 10^{-6})	Cross linker conc. (mole × 10^{-3})	Monomer conc. (mole × 10^{-2})	% Cross linking	pH 1.4	pH 6.8	pH 7.4
Dxt-g-p(HEMA) 1	0.36992	0.6486	7.684	61.97	230 ± 7	255 ± 7	280 ± 3
Dxt-g-p(HEMA) 2	0.92480	0.6486	7.684	83.42	175 ± 4	189 ± 6	194 ± 3
Dxt-g-p(HEMA) 3	1.84960	0.6486	7.684	71.37	194 ± 7	205 ± 7	224 ± 7
Dxt-g-p(HEMA) 4	0.92480	0.9729	7.684	87.67	165 ± 2	180 ± 1	186 ± 1
Dxt-g-p(HEMA) 5	0.92480	1.2972	7.684	91.08	150 ± 3	174 ± 4	184 ± 1
Dxt-g-p(HEMA) 6	0.92480	1.6215	7.684	82.08	181 ± 5	200 ± 8	210 ± 3
Dxt-g-p(HEMA) 7	0.92480	1.2972	9.605	80.08	187 ± 3	195 ± 3	215 ± 2

then reweighed. The equilibrium swelling was attained at ~5 h. The % ESR has been calculated using eqn (1):

$$\text{ESR } (\%) = \frac{W_{eq} - W_d}{W_d} \times 100 \quad (1)$$

W_{eq} is the weight of hydrogel at equilibrium and W_d is the weight of dried hydrogel.

For swelling kinetics, water absorption of the hydrogels has been measured at consecutive time intervals until and unless equilibrium was achieved. The pH-sensitivity of the hydrogel was determined using the equilibrium swelling ratio in various buffer media. The Voigt model (eqn (2)) is used to find out the swelling rate of the hydrogel.[16,19]

$$S_t = S_e(1 - e^{-t/\tau}) \quad (2)$$

where S_t (g g^{-1}) is the swelling at time t, S_e (g g^{-1}) is the equilibrium swelling, t is the time (min) for swelling and τ (min) stands for the rate parameter. The rate parameter (τ) has been determined using eqn (2), which is a measure of the swelling rate *i.e.* the lower the rate parameter value (τ) the higher be the swelling rate.[19]

2.5 *In vitro* cell compatibility

The powdered samples were made into pellets for assessing cell viability and proliferation. The pellets were sterilized using 70% alcohol and UV followed by washing with sterilized PBS, pH 7.4. HaCat cell line (NCCS, Pune) was cultured in 5% CO_2 atmosphere at 37 °C (Heracell 150i, Thermo, USA) in DMEM (Himedia) supplemented with 10% foetal bovine serum, 1% antibiotics, 3.7% sodium bicarbonate, and 1% L-glutamine (all Himedia). The cells were harvested from tissue culture flasks using 0.25% trypsin in 1 mM EDTA (Himedia) and plated onto pellets. To seed similar cell density, cell suspension was counted using a Countess (Invitrogen, USA). 10^4 cells were plated on both samples and wells of a tissue culture plate (TCP).

Cell proliferation and viability. MTT [3-(4,5-dimethylthiazol-2-yl)-2,5-diphenyltetrazolium bromide] assay of the adherent HaCaT cells on the pellets was examined after 1, 3 and 5 days. After predetermined time intervals, culture medium was discarded, washed thoroughly with PBS and incubated with 5 mg mL^{-1} MTT solution (Sigma, US) at 37 °C for 4 h. The insoluble formazan crystals formed were allowed to dissolve in dimethyl sulfoxide and absorbance was read in 96-well plates at 570 nm on a microplate reader (RMS Instruments, India).

2.6 Preparation of hydrogel based tablets and *in vitro* drug release study

The Dxt-g-p(HEMA) hydrogel (450 mg) was finely ground in a blender, with a binder, PVP-K30 (50 mg) and ornidazole drug (500 mg). The mixture was wet with ethanol and mixed further. The paste was dried at 40 °C to a constant weight. Then a mixture of silicon dioxide and magnesium stearate (2 : 1 ratios) was added as a lubricant, in an amount not exceeding 3% of the ground powder. After mixing and sieving (20 meshes), tablets of 1 g each were prepared by compression in a tablet punching machine at a pressure of 2–3 t per cm^2.

During drug release, some tablets disintegrated partially. The degree of erosion (D) was calculated using eqn (3), based on the difference between the initial dry weight of the tablet (W_i) and the dry weight of the tablet ($W_{d(t)}$) at time t, considering the initial amount of drug in tablet (W_d) and fraction of drug release at time t (M_t/M_∞),

$$D(t)(\%) = \frac{W_i - W_{d(t)} - W_d(1 - M_t/M_\infty)}{W_i} \times 100 \quad (3)$$

The *in vitro* release of entrapped drug (*i.e.* ornidazole) from the hydrogels was determined using standard Dissolution Test Apparatus (Lab India, Model: DS 8000), under a constant rotation of 60 rpm at 37 ± 0.5 °C using 900 mL simulated gastric fluid (SGF, pH 1.2) for 2 h, phosphate buffer having pH 6.8 for the next 3 h and subsequently in 900 mL of simulated intestinal fluid (SIF, pH 7.4) for a further 13 h. Aliquots were withdrawn from the release media after every 60 min and replaced by an equal volume at each sampling time. The amount of drug release was measured with the help of UV-Visible spectrophotometer (Shimadzu, Japan; Model – UV 1800).

To determine the release kinetics and mechanism of the drug release, various mathematical models were used such as the zero order kinetic model, first order kinetic model, Korsemeyar–Peppas model, Higuchi model, Hixson–Crowell model and nonlinear Kopcha model.

Drug stability study. Finally a tablet containing ornidazole underwent an accelerated stability study for three months to confirm the stability of the drug in the present hydrogel matrix *i.e.* Dxt-g-p(HEMA) 5. It is essential to find out the compatibility in accelerated conditions. A tablet was packed in a glass bottle and placed in the humidity chamber where the temperature was kept at 40 ± 2 °C and relative humidity (RH) was maintained at 75 ± 5% throughout the study period.

3. Results and discussions

3.1 Synthesis of Dxt-g-poly(HEMA) based hydrogel

Poly(HEMA) has been grafted onto dextrin backbone in the presence of KPS as initiator and MBA as cross linker in an inert atmosphere of nitrogen. An expected explanation for the formation of the graft copolymer hydrogel is based on the assumption that KPS generates free radical sites on dextrin. In the presence of cross linker MBA, because of its poly-functionality, a new macro-radical was formed that has four reactive sites[20] and these sites can be linked with the radical generated on dextrin grafted poly(HEMA) backbone as shown in Scheme 1. This results in the formation of a three dimensional cross linked hydrogel. In order to observe the effect of reaction parameters, several grades of hydrogels have been prepared (Table 1) and the best one has been selected with respect to its higher % cross linking (% CE) and lower equilibrium swelling (% ESR).

Effect of reaction parameters. For hydrogels *i.e.* Dxt-g-p(HEMA) 1 to Dxt-g-p(HEMA) 3, the initiator concentration was varied from 0.36992 × 10^{-6} mol to 1.84960 × 10^{-6} mol (Table 1)

and it has been found that the Dxt-g-p(HEMA) 2 hydrogel has lower % ESR *i.e.* higher cross linking ratio. This is due to the fact that, with relatively low initiator concentration, only a few grafting sites would be generated on the polysaccharide backbone, which will expand the length of the grafted/cross linked chains to a large extent and hence the cross linking ratio would be higher.

The cross linker concentration was varied from 0.6486×10^{-3} mol to 1.6215×10^{-3} mol (Table 1) and maximum cross linking was obtained (*i.e.* minimum % equilibrium swelling) with a MBA concentration of 1.2972×10^{-3} mol. This is because the higher the amount of cross linker incorporated in the hydrogel structure, the higher will be the cross linking ratio. For this reason, the hydrogel structure will be more rigid and will swell less compared to the same hydrogel with a lower cross linking ratio.[14]

It has been found that with an increase in monomer conc. (*i.e.* HEMA) from 7.684×10^{-2} mol to 9.605×10^{-3} mol, the % ESR increased, which implied that the amount of cross linking is less (Table 1). This may be because of the formation of more homopolymer (which has been separated from the hydrogel during the synthesis process) with higher monomer concentration.

3.2 Characterization of hydrogel

From the FTIR spectrum of dextrin (Fig. 1a), it has been observed that the peak at 3393 cm^{-1} is due to the stretching vibrations of O–H, a small peak at 2928 cm^{-1} is attributed to the C–H stretching vibrations. The peaks at 1026 and 931 cm^{-1} are assigned to the C–O–C stretching vibrations. Fig. 1b shows the FTIR spectrum of the synthesised hydrogel [Dxt-g-p(HEMA) 5]. The O–H stretching band of dextrin and the N–H stretching band of the cross linker (*i.e.* MBA) overlap with each other and lead to a broad peak appearing at 3464 cm^{-1}. Two intense peaks at 1735 and 1153 cm^{-1} are attributed to the stretching frequency of the ester group (*i.e.* C=O and C–O) and the peak 2952 cm^{-1} is due to C–H stretching of the $-CH_3$ group, which indicates the presence of poly(HEMA) on the dextrin backbone. Two peaks at 1642 and 1491 cm^{-1} are due to the amide-I and amide-II bands of MBA and one peak at 1397 cm^{-1} indicates the presence of C–N group which verifies the existence of the cross linker (*i.e.* MBA) in the polymer matrix.

In the FTIR spectrum of ornidazole (Fig. 1c), peaks at 3314 and 3172 cm^{-1} are due to the –O–H stretching mode and C–H stretching mode respectively. For asymmetric NO_2 stretching, the peak appears at 1539 cm^{-1}. The peaks at 1365–1270 cm^{-1} are due to the symmetric stretching mode of the NO_2 group. The peak at 1153 cm^{-1} is due to the C–O stretching vibration. The peaks at 829 and 742 cm^{-1} are attributed to C–N *i.e.* the carbon atom connected with an NO_2 group and stretching frequency of C–Cl bond vibration respectively. In the spectrum of the triturated form of the ornidazole tablet (Fig. 1d), the carbonyl group stretching frequency shifted from 1735 cm^{-1} to 1665 cm^{-1}, amide-I from 1642 cm^{-1} to 1531 cm^{-1} and N–H stretching shifts from 3464 cm^{-1} to 3393 cm^{-1} which signify that the interaction between hydrogel and drug is through H-bonding as shown in Fig. 2.

XRD analysis was carried out to investigate the drug's polymorphism after tablet formation. XRD profiles of cross linked hydrogel, ornidazole and triturated form of ornidazole tablet are shown in Fig. 3. In the case of the cross linked hydrogel (Fig. 3a), a broad characteristic peak appeared in $2\theta = 18^\circ$ which indicates that cross linked hydrogel is amorphous in nature. Ornidazole (Fig. 3b) showed peaks at $2\theta = 13.5^\circ$, 16.2°, 21.1°, 23.2°, 24.4°, 25.8°, 27.6°, 30.7°, 32.6° because of its close molecular packing and regular crystallization structure. From the X-ray diffraction pattern of the ornidazole loaded tablet (Fig. 3c), it has been observed that the peak of cross linked

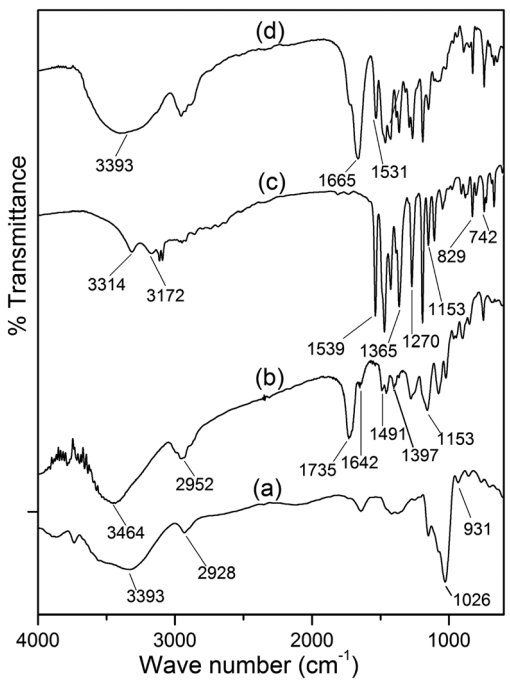

Fig. 1 FTIR spectra of (a) dextrin, (b) Dxt-g-p(HEMA) 5 hydrogel, (c) ornidazole, and (d) triturated form of ornidazole tablet.

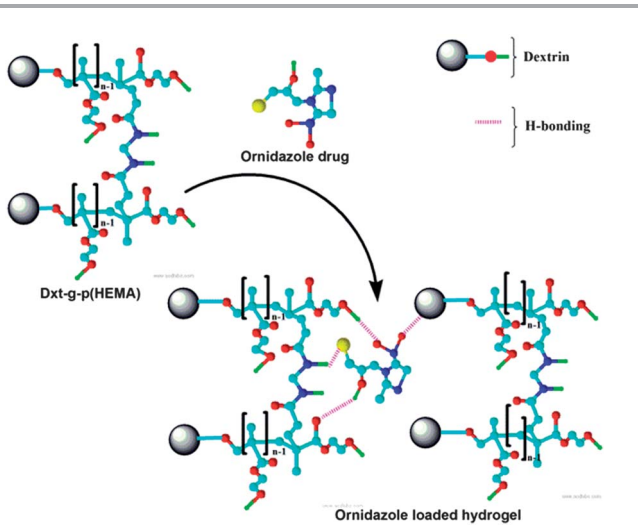

Fig. 2 Interaction between ornidazole drug and the hydrogel.

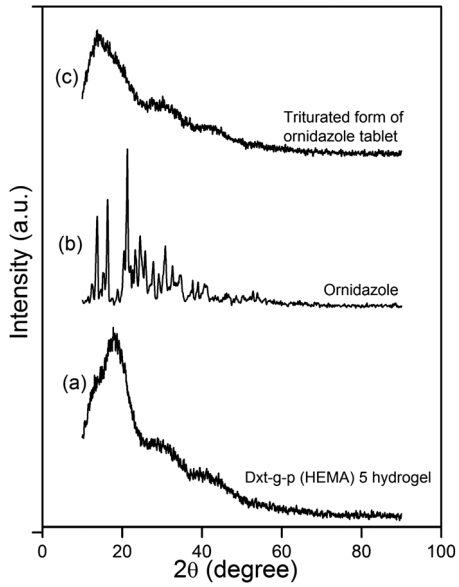

Fig. 3 XRD profile of (a) Dxt-g-p(HEMA) 5 hydrogel, (b) ornidazole and (c) triturated form of ornidazole tablet.

hydrogel shifted towards a lower 2θ value (*i.e.* to 13.7°). This shifting indicates the molecular level dispersion of ornidazole drug in the hydrogel matrix.[21] Also, the XRD of the tablet formulation emphasizes the existence of good compatibility between the drug and the excipients.[21]

The CHN analyses of dextrin (% C – 39.65, % H – 6.83, % N – 0.00) and Dxt-g-p(HEMA) 5 (% C – 52.81, % H – 8.61, % N – 0.37) depict that there is substantial enhancement of amount of carbon, hydrogen and nitrogen in the hydrogel. The increase in % C and % H is because of the presence of poly(HEMA) chains in the hydrogel network. However, an increase in % N corroborates the presence of MBA as cross linker in the hydrogel structure.

The ^{13}C NMR spectra of dextrin and Dxt-g-p(HEMA) 5 are shown in Fig. 4. The NMR spectrum of dextrin (Fig. 4a) has four characteristics peaks at $\delta = 111.4$, 88.5, 79.4, and 68.1 ppm, which are attributed to the anomeric carbon atom, carbon atom of CH_2OH group, carbon atom connected by –OH group in the six member ring except for the anomeric carbon atom (*i.e.* C_2–C_4) and C_5 carbon atom respectively. In comparison to dextrin, the cross linked hydrogel has few additional peaks. The peak at 179.2 ppm correlates to the carbonyl carbons, which originate from the cross linker as well as from poly(HEMA). Peaks at 55.9 and 17.1 ppm are assigned to the carbon atom connected with –OH and methyl carbon of poly(HEMA). Another peak at 45.8 ppm can be assigned to sp^3 hybridized carbon atom, which has been formed during polymerization of HEMA (*i.e.* two sp^2 hybridized carbon atoms of HEMA monomer shifted to sp^3 hybridized carbon atoms during polymerization). Thus, the NMR result confirms that poly(HEMA) has been grafted onto the dextrin backbone in the presence of MBA as cross linker.

The surface morphologies of dextrin and Dxt-g-p(HEMA) 5 are shown in Fig. 5. Dextrin (Fig. 5a) has a fine oval shaped granular morphology. However, after modification, the granular appearance of dextrin is distorted and the morphology of the hydrogel became porous (Fig. 5b). The incorporation of poly(HEMA) and cross linker onto dextrin backbone affects the cross link ratio as well as the structure of the hydrogel, leading to a change of microstructure of modified dextrin based hydrogel. Due to numerous interconnected pores in the hydrogel network, water molecules can easily spread and hence affect the rate of swelling. It is also expected that these pores are the regions of water permeation and interaction sites of external stimuli like pH, temperature, ionic strength *etc.*

Thermogravimetric analysis of dextrin (Fig. 6a) and Dxt-g-p(HEMA) 5 (Fig. 6b) hydrogel explain the different thermal decomposition mechanisms. Dextrin has two different zones of weight loss. The initial decomposition may be because of the traces of moisture present. The second weight loss region

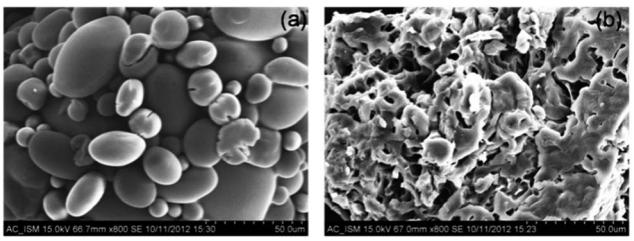

Fig. 5 SEM micrograph (magnification × 800) of (a) dextrin, (b) Dxt-g-p(HEMA) 5 hydrogel.

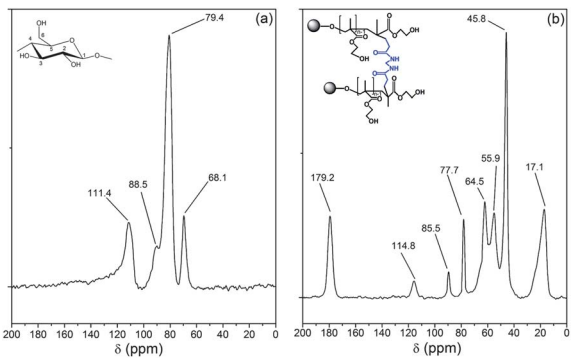

Fig. 4 ^{13}C NMR spectra of (a) dextrin, (b) Dxt-g-p(HEMA) 5 hydrogel.

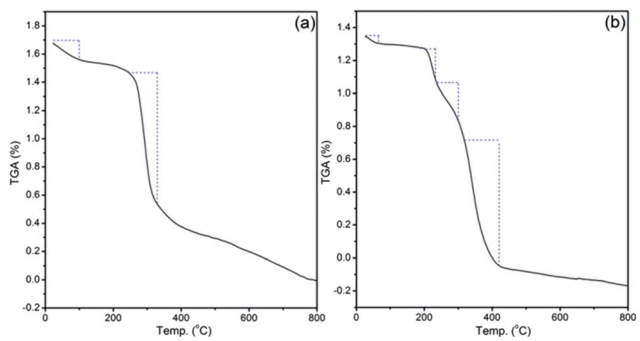

Fig. 6 Thermogravimetric analysis of (a) dextrin, (b) Dxt-g-p(HEMA) 5 hydrogel.

(258–330 °C) is due to the degradation of the polysaccharide backbone. In contrast to dextrin, the hydrogel has two additional weight loss regions; one is in between 205 and 230 °C, due to the degradation of the presence of cross linker in the hydrogel structure and another extra zone is in the region of 350–440 °C, which is owing to the degradation of the poly-(HEMA) present in the hydrogel structure. The presence of these extra zones of weight loss supports the presence of MBA as well as poly(HEMA) in the hydrogel structure.

Cell attachment, viability and proliferation indicate cellular compatibility towards a material. An MMT reduction assay was used to determine cell viability after 1, 3, 5 days (Fig. 7). The Dxt-g-p(HEMA) 5 hydrogel as well as tissue culture plate (TCP) maintained a viable population of HaCaT cells throughout the study period (Fig. 7a). No significant differences were seen on the 1st day of cell seeding. However, after 3 days of culture, the hydrogel showed significantly higher viability than TCP.

Thus, the synthesized material is not toxic for HaCaT cells. The absorbance values were further converted to rate of cell proliferation using a standard curve. After 5 days, the no. of cells on Dxt-g-p(HEMA) 5 hydrogel and TCP were $4.29 \pm 0.18 \times 10^4$ and $3.21 \pm 0.19 \times 10^4$, respectively (Fig. 7b). This may be because the hydrogel being hydrophilic in nature, swells to form a three dimensional structure that provides more surface area for cells to attach and proliferate whereas cell proliferation is restricted on a two dimensional surface like TCP.

3.3 Swelling characteristics of hydrogel

The equilibrium swelling properties of dextrin and various hydrogels were investigated at pH 1.2, 6.8 and 7.4 buffer solutions at 37 °C temperature. It has been observed that dextrin shows a declining trend of swelling with time which is because of its solubility in aqueous solution. The hydrogel attained its equilibrium swelling at ~5 h (Fig. 8). It is obvious that the hydrogels demonstrate a faster swelling rate. This observation can be explained by the fact that the presence of poly(HEMA) and MBA in the hydrogel structure enhances the hydrophilicity of the network and facilitates the hydration as well as expansion of the network. In addition to that, the porous morphology of the hydrogel also enhances the diffusion of water into the hydrogel network. However, out of various hydrogels, Dxt-g-p(HEMA) 5 shows the lowest equilibrium swelling (Table 1 & Fig. 8) because of its maximum cross linking ratio (Table 1), which will make the hydrogel structure more rigid and hence will swell less as compared to same hydrogel having a lower cross linking ratio.

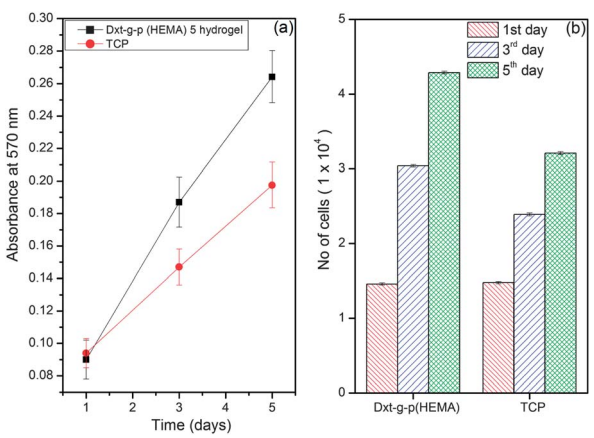

Fig. 7 Cell viability study of Dxt-g-p(HEMA) 5 hydrogel.

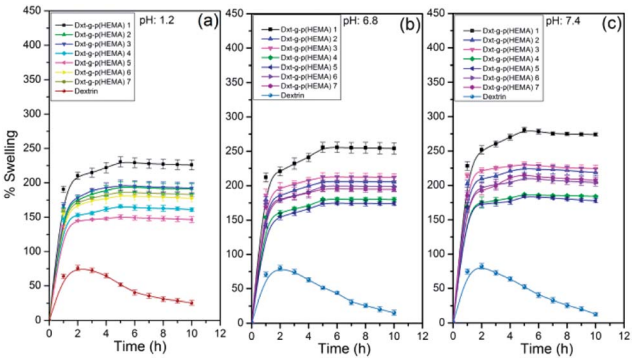

Fig. 8 Swelling characteristic of dextrin and various hydrogels at (a) pH 1.2 (b) pH 6.8 and (c) pH 7.4 (results represented are mean ± SD, $n = 3$).

As obvious from Fig. 8, all hydrogels show pH dependent swelling behaviour. This may be because of the fact that, at acidic pH (*i.e.* pH 1.2), the hydrophilic groups present in the hydrogel network get protonated which hindered the formation of H-bonding with water. This will result in less swelling compared to pH 7.4. However, at pH 7.4, all the hydrophilic groups remain free and thus able to form more H-bonding with the media. This would facile the penetration of a large no of water molecules into the hydrogel network, making the swelling higher.

Swelling kinetics. From the swelling curve (Fig. 8), it has been found that initially the rate of water adsorption by Dxt-g-p(HEMA) hydrogels increases sharply and then begins to level off. Afterwards, it reaches an equilibrium state ~5 h. The data has been fitted with a Voigt model according to eqn (2) and the rate parameter (τ) values have been determined and reported in Table 2. Since, τ is a measure of swelling rate, it is useful to find out the comparative evaluation of the rate of water absorption on various hydrogels. It is apparent from Table 2 that Dxt-g-p(HEMA) 5 has the highest τ value in various pH media. Hence this composition has the lowest swelling rate. It is also obvious

Table 2 Swelling kinetics parameter

	Value of rate parameter		
Polymer	pH 1.2	pH 6.8	pH 7.4
Dxt-g-p(HEMA) 1	143.06	109.64	78.24
Dxt-g-p(HEMA) 2	153.84	115.47	83.68
Dxt-g-p(HEMA) 3	145.56	112.48	83.19
Dxt-g-p(HEMA) 4	187.26	123.45	105.59
Dxt-g-p(HEMA) 5	259.74	123.76	106.04
Dxt-g-p(HEMA) 6	185.87	123.30	104.71
Dxt-g-p(HEMA) 7	164.47	120.91	99.30

that the rate parameter (τ) value is lower (Table 2) in pH 7.4 as compared to pH 6.8 and pH 1.2. The decrease in rate parameter of cross linked hydrogels with increase of the pH from acidic to alkaline media indicates the faster swelling rate in alkaline media. In acidic media *i.e.* at pH 1.2, a large no of the hydrophilic groups present in Dxt-g-p(HEMA) hydrogel get protonated, which opposes the formation of H-bonding with water molecules and consequently the swelling value decreases. However, at pH 6.8 or at mild alkaline media (*i.e.* in pH 7.4), hydrophilic groups of Dxt-g-p(HEMA) hydrogels remain in the unprotonated state, and thus interact with a large no of water molecules. This will result in an enhancement of the swelling capacity. This responsiveness and fast swelling behaviour may be of significant importance in case of colon specific drug delivery system.

3.4 *In vitro* drug release studies

The cumulative percentage of ornidazole release from various hydrogels as well as from dextrin as a function of time is shown in Fig. 9.The chemical structure of the hydrogel affects the drug release behaviour.[22] The release rate of the drug is directly proportional to the equilibrium swelling ratio of the hydrogels.[12] The higher swelling ratio of hydrogels creates a larger surface area for diffusion of the drug from the inside of the hydrogel to the environment.[12] In particular, the release of water soluble drugs from hydrogels occurs only after penetration of water into the hydrogel network, which will swell and dissolve the drug, followed by drug diffusion.[12] It is obvious from Fig. 9 that the rate of drug release is higher at pH 6.8 and pH 7.4 than that at pH 1.2. This may be because of the fact that at pH 1.2, the network hydrogel is in a collapsed state, resulting in a lower rate of swelling and hence the drug was unable to diffuse from the hydrogels. However, at higher pH, the hydrogels swelled rapidly, leading to an increase in drug diffusion from the matrix. Out of various hydrogels, Dxt-g-p(HEMA) 5 showed more sustained drug release (~68.7% release after 18 h) behaviour.

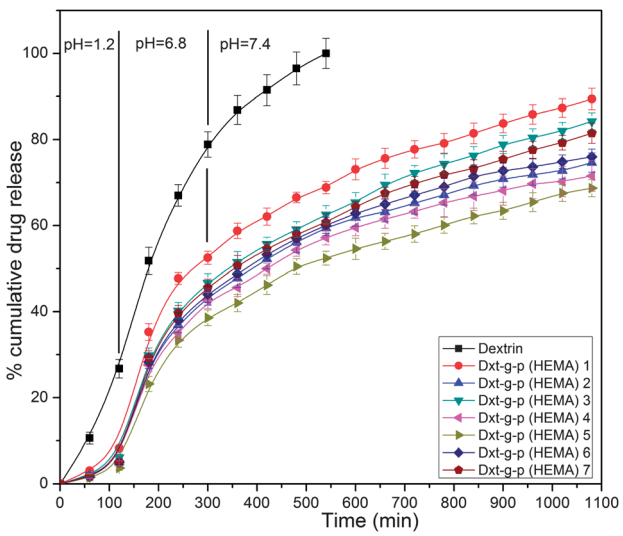

Fig. 9 Drug release profile of dextrin and various hydrogels at pH 1.2, 6.8 and 7.4 for 2 h, 3 h and 13 h respectively (results represented are mean ± SD, $n = 3$).

Table 3 % Erosion of dextrin and various hydrogels (results represented here are mean ± SD, $n = 3$)

	% Erosion (ornidazole tablet)	
Hydrogel	pH 6.8	pH 7.4
Dextrin (Dxt)	76.12 ± 4.23	80.35 ± 5.25
Dxt-g-p(HEMA) 1	24.01 ± 2.34	27.16 ± 3.20
Dxt-g-p(HEMA) 2	19.81 ± 1.18	21.70 ± 3.25
Dxt-g-p(HEMA) 3	20.06 ± 1.02	21.79 ± 3.12
Dxt-g-p(HEMA) 4	16.11 ± 1.14	18.09 ± 2.25
Dxt-g-p(HEMA) 5	12.61 ± 2.88	15.54 ± 4.32
Dxt-g-p(HEMA) 6	17.00 ± 1.19	18.99 ± 2.80
Dxt-g-p(HEMA) 7	17.89 ± 3.86	19.57 ± 4.25

Further, it has been observed that the rate of erosion (Table 3) of different hydrogels is much lower in comparison with dextrin, which also has a direct impact on the rate of drug release.

Thus, the results suggested that ornidazole was released in a controlled manner from modified dextrin based hydrogels. This observation indicates that the presence of poly(HEMA) as well MBA in the hydrogel structure enhances the hydrophilicity of the network and thus causing the release of the enclosed drug in a more sustained way.

Evaluation of drug release kinetics and drug release mechanism. To investigate the drug release kinetics and mechanism of drug release from modified dextrin based hydrogels, the release data were analyzed using zero order, first order, Higuchi, Hixson–Crowell, Korsemeyar–Peppas and Kopcha models. Since, no single model successfully predicts the release kinetics as well as the release mechanism of the drug from a hydrogel matrix; various mathematical models have been used to explain the experimental observations during drug release.

Drug release kinetics. To analyze the *in vitro* release data and evaluate the release kinetics, zero order and first order kinetic models have been used. The zero order kinetic model (eqn (4)) explains the drug dissolution from transdermal systems, as well as matrix tablets with low soluble drugs, coated forms, osmotic systems, *etc.*[23]

$$Q_t = Q_0 + K_0 t \quad (4)$$

where Q_t is the amount of drug release in time t, Q_0 the initial amount of drug in solution (most times, $Q_0 = 0$) and K_0 is the zero order release constant expressed in units of concentration/time and t is the time.

On the other hand, the first order kinetic model (eqn (5)) describes the release from systems containing water soluble drugs in porous matrices, where the drug release is proportional to the amount of drug remaining in the interior of the matrix.[24]

$$\log Q_t = \log Q_0 + \frac{K_1 t}{2.303} \quad (5)$$

where, Q_t, Q_0 is the amount of drug released in time t and the amount of initial drug in tablet respectively, K_1 is first order rate constant.

Here, the *in vitro* release of ornidazole from hydrogels was executed in various buffer solutions (Fig. 9). It has been

observed that the release follows a first order kinetic model than that of zero order kinetic model (based on higher R^2 value, Table S1, see ESI†).

Mechanism of drug release. In the hydrogel system, absorption of water from the dissolution media changes the dimension and physicochemical properties of the hydrogel which facilitates the drug release from hydrogel matrices. For controlled release of drug, the release should follow three steps. First is the penetration of the dissolution media into the tablet matrix (hydration). The second step is the polymer relaxation or erosion of the matrix and the third one is the transport of the dissolved drug, either through the hydrated matrix or from the parts of the eroded tablet to the surrounding dissolution medium.[25] On the basis of diffusion of water into the hydrogel matrix three types of diffusion mechanism of drug from polymer based matrix have been proposed: Fickian diffusion, non-Fickian diffusion and case II diffusion.[26]

The Korsemeyar–Peppas model (eqn (6)) is very crucial to find out the mechanism of drug release from a polymer matrix.[27] This model applies up to 60% of the total amount of drug released.

$$\frac{M_t}{M_\infty} = Kt^n \tag{6}$$

where M_t/M_∞ is the fractional release of drug at time t, 'k' is the constant characteristic of a drug–polymer system and 'n' is the diffusion exponent. The 'n' value is used to characterize different release mechanisms. $n \leq 0.45$ indicates Fickian diffusion, in which the rate of diffusion is less than that of relaxation. The value of 'n' in the range of $0.45 < n < 0.89$ indicates the mechanism is non-Fickian diffusion or anomalous diffusion, where the diffusion and relaxation rates are comparable. When $n > 0.89$, the major mechanism of drug release is case II diffusion (relaxation-controlled transport) where diffusion is very rapid compared to the relaxation process of the polymer.

The Higuchi model (eqn (7)) illustrates the release of drugs as a diffusion process from an insoluble matrix based on Fick's law.[28]

$$Q_t = Q_0 + K_H t^{1/2} \tag{7}$$

Where, Q_t is the amount of drug release in time t, Q_0 the initial amount of drug in solution, K_H is the Higuchi dissolution constant.

The Hixson–Crowell cube root law (eqn (8)) exemplifies the release from systems when there is a change in surface area and diameter of particles or tablets, which supports that the rate of erosion of the matrix is the main principle of drug release.[29]

$$W_0^{1/3} - W_t^{1/3} = K_{HC} t \tag{8}$$

where, W_t is the amount of drug release after time t, W_0 is the initial amount of the drug in tablet and K_{HC} is the rate constant for Hixson–Crowell rate equation.

The Kopcha model (eqn (9)) is also used to quantify the relative contributions of diffusion and polymer relaxation to drug release.[30]

$$Q_t = At^{1/2} + Bt \tag{9}$$

where, 'A' is the diffusional exponent and 'B' is the erosional exponent. If 'A' is much greater than 'B' then the ratio of the exponents A/B will be very high, suggesting that the drug release from matrix is primarily controlled by a Fickian diffusion process.

To understand the mechanism of drug release, we have used the Korsemeyar–Peppas model in both media (*i.e.* pH 6.8 and pH 7.4). It has been found that the 'n' value lies between 0.45 and 0.89 (Table S1, see ESI†), which clearly indicates that the drug release from Dxt-g-p(HEMA) based hydrogels follows a non-Fickian diffusion mechanism *i.e.* the drug release depends on both a diffusion process as well as a polymer relaxation *i.e.* erosion process.

Further it has also been observed that comparable linearity was found in both media in the case of the Higuchi model ($R^2 =$ 0.9810–0.9968 in pH 6.8, $R^2 = 0.9824$–0.9960 in pH 7.4) (Table S1, see ESI†). Consequently release follows the Higuchi model which supports that the drug release is controlled by a diffusion process.

The release mechanism was further confirmed by calculating the diffusion exponent (A) and erosion exponent (B) derived from the nonlinear fitted Kopcha model. The calculated value of 'A' and 'B' indicates both factors (diffusion and erosion) are responsible for drug release (Table S1, see ESI†). In pH 6.8, the value of 'A' is greater than 'B' which states that in this medium drug release is quantitatively controlled by a diffusion process rather than an erosion process. On the other hand at pH 7.4, the value of both 'A' and 'B' are comparable which clarifies that the drug release is controlled by both diffusion as well as polymer relaxation.

Stability study. A stability study of the final ornidazole tablet was performed. The justification for stability testing is to find out how the quality of a tablet varies with time under the influence of various environmental factors like temperature, humidity *etc.*[31] It is evident from the results [Table S2 and Fig. S1 (FTIR analysis), Fig. S2 (XRD analysis), Fig. S3 (release characteristics – initially and after 3 months) see ESI†] that the drug stability using Dxt-g-p(HEMA) 5 hydrogel as carrier for ornidazole is ~98% up to 3 months.

Considering all the shortcomings of reported hydrogels as well as colon specific ornidazole delivery systems regarding biodegrability, cytotoxicity, compatibility and stability (as mentioned in introduction section), the developed Dxt-g-p(HEMA) hydrogel is novel. Use of Dxt-g-p(HEMA) for colon specific ornidazole delivery is advantageous over reported systems due to (a) excellent swelling properties, (b) non-cytotoxicity, (c) release in a more sustained way (~68.7% even after 18 h). The last one is the most important prerequisite for pharmaceutical application, as slow release of ornidazole may prevent any severe side effects. Moreover, % of drug stability using Dxt-g-p(HEMA) hydrogel as carrier for ornidazole is ~98% up to 3 months, which is quite promising and restricts the degradation of the drug in the stomach region.

4. Conclusions

A series of cross linked hydrogels, composed of dextrin and poly(HEMA), were synthesized *via* free radical polymerization technique. Through introducing poly(HEMA) onto a dextrin

backbone, the porous structure of a hydrogel was achieved and the hydrophilicity was increased. Compared with pure dextrin, the hydrogels exhibited enhanced thermal stability and faster swelling rates. The results confirm that the prepared hydrogel shows good biocompatibility, being also able to effectively stimulate cell proliferation. Further, the hydrogel demonstrates excellent potential as a novel matrix for controlled release of ornidazole in colonic region in a controlled and sustained way. The drug release from dissolution media follows a first order kinetic model and non-Fickian type diffusion mechanism. Finally, the developed hydrogel is probably a better candidate for pharmaceutical applications, in particular for colon specific ornidazole release.

Acknowledgements

The first author wishes to acknowledge University Grant Commission, New Delhi, India (Ref. no.19-06/2011(i) EU-IV; Sr. no. 2061110303, Dated: 30.11.2011) for providing financial assistance Under Junior Research Fellowship Scheme. The authors acknowledge the financial support from Department of Science and Technology, New Delhi, India in form of a research grant (NO:SR/FT/CS-094/2009) to carry out the reported investigation. The authors also acknowledge the kind help of Dr Animesh Ghosh, Department of Pharmaceutical Sciences, BIT, Mesra, Ranchi, India for providing drug stability study.

Notes and references

1 (*a*) T. Coviello, P. Matricardi, C. Marianecci and F. Alhaigue, *J. Controlled Release*, 2007, **119**, 5–24; (*b*) L. Pescosolido, T. Piro, T. Vermonden, T. Coviello and F. Allhaique, *Carbohydr. Polym.*, 2011, **86**, 208–213; (*c*) A. S. Hoffman, *Adv. Drug Delivery Rev.*, 2002, **54**, 3–12.

2 (*a*) P. Kurian and J. P. Kennedy, *J. Polym. Sci., Part A: Polym. Chem.*, 2002, **40**, 1209–1217; (*b*) A. Finne and A. C. Albertsson, *J. Polym. Sci., Part A: Polym. Chem.*, 2003, **41**, 1296–1305; (*c*) B. V. Slaughter, S. S. Khurshid and O. Z. Fisher, *Adv. Mater.*, 2009, **21**, 3307–3329; (*d*) N. A. Peppas, J. Z. Hilt and A. Khademhosseini, *Adv. Mater.*, 2006, **18**, 1345–1360.

3 (*a*) M. Hamidi, A. Azadi and P. Rafiei, *Adv. Drug Delivery Rev.*, 2008, **60**, 1638–1649; (*b*) E. Soussan, S. Cassel and M. Blanzat, *Angew. Chem., Int. Ed.*, 2009, **48**, 274–288; (*c*) L. Pan, Q. He, J. Liu, Y. Chen, M. Ma, L. Zhang and J. Shi, *J. Am. Chem. Soc.*, 2012, **134**, 5722–5725; (*d*) L. Tang, T. M. Fan, L. B. Borst and J. Cheng, *ACS Nano*, 2012, **6**, 3954–3966.

4 (*a*) J. A. Killion, L. M. Geever, D. M. Devine, J. E. Kennedy and C. L. Higginbotham, *J. Mech. Behav. Biomed. Mater.*, 2011, **4**, 1219–1227; (*b*) S. G. Lee, G. F. Brunello, S. S. Jang and D. G. Bucknall, *Biomaterials*, 2009, **30**, 6130–6141; (*c*) H. Shin, B. D. Olsen and A. Khademhosseini, *Biomaterials*, 2012, **33**, 3143–3152.

5 (*a*) Z. Liu, Y. Jiao, Y. Wang, C. Zhou and Z. Zhang, *Adv. Drug Delivery Rev.*, 2008, **60**, 1650–1652; (*b*) S. A. Agnihotri, N. N. Mallikarjuna and T. M. Aminabhavi, *J. Controlled Release*, 2004, **100**, 5–28; (*c*) B. K. Nanjawade, F. V. Manvi and A. S. Manjappa, *J. Controlled Release*, 2007, **122**, 119–134; (*d*) M. D. M. Ortega, C. A. Lorenzo, A. Concheiro and T. Loftsson, *Int. J. Pharm.*, 2012, **428**, 152–163; (*e*) C. He, L. Yin, C. Tang and C. Yin, *Biomaterials*, 2013, **34**, 2843–2854.

6 (*a*) J. O. Karlsson and P. Gatenholm, *Polymer*, 1997, **38**, 4727–4731; (*b*) K. Pal, A. K. Banthia and D. K. Majumdar, *Des. Monomers Polym.*, 2009, **12**, 197–220; (*c*) N. A. Peppas, P. Bures, W. Leobandung and H. Ichi, *Eur. J. Pharm. Biopharm.*, 2000, **50**, 27–46; (*d*) Y. Qiu and K. Park, *Adv. Drug Delivery Rev.*, 2001, **53**, 321–339.

7 (*a*) W. F. Zambuzzi, C. V. Ferreira, J. M. Granjeiro and H. Aoyama, *J. Biomed. Mater. Res., Part A*, 2011, **97**, 375–382; (*b*) L. Zhang, J. Rodriguez, J. Raez, A. J. Myles, H. Fenniri and T. J. Webster, *Nanotechnology*, 2009, **20**, 175101.

8 (*a*) S. S. Vaghani, M. M. Patel and C. S. Satish, *Carbohydr. Res.*, 2012, **347**, 76–82; (*b*) B. Singh and M. Vashistha, *Nucl. Instrum. Methods Phys. Res., Sect. B*, 2008, **266**, 2009–2020; (*c*) P. Patel, A. Roy, V. K. SM and M. Kulkarni, *Int. J. Drug Dev. Res.*, 2011, **3**, 52–61; (*d*) B. Singh and N. Sharma, *Colloids Surf., B*, 2011, **82**, 325–332; (*e*) M. R. Saboktakin, R. M. Tabatabaie, A. Maharramov and M. A. Ramazanov, *Int. J. Biol. Macromol.*, 2011, **48**, 381–385.

9 D. A. Talan, K. G. Naber, J. Palou and D. Elkharrat, *Int. J. Antimicrob. Agents*, 2004, **23**, 54–66.

10 Y. S. R. Krishnaiah, P. R. Bhaskar Reddy, V. Satyanarayana and R. S. Karthikeyan, *Int. J. Pharm.*, 2002, **236**, 43–55.

11 T. S. Anirudhan, S. Sandeep and P. L. Divya, *RSC Adv.*, 2012, **2**, 9555–9564.

12 P. Singh, R. Mittal, G. C. Sharma, S. Singh, A. Singh, *In profiles of Drug Substances, and Excipients, and Related Methodology*, ed. H. G. Brittain, Academic Press: New York, 2006, vol. 30, pp. 123–184.

13 J. K. Oh, D. I. Lee and J. M. Park, *Prog. Polym. Sci.*, 2009, **34**, 1261–1282.

14 (*a*) T. Asoh, T. Kaneko, M. Matsusaki and M. Akashi, *J. Controlled Release*, 2006, **110**, 387–394; (*b*) S. Geresh, J. Peisahov, J. Voorspoels, J. P. Remon and J. Kost, *Biomed. Health Res.*, 1998, **16**, 192–196; (*c*) S. Geresh, G. Y. Gdalevsky, I. Gilboa, J. Voorspoels, J. P. Remon and J. Kost, *J. Controlled Release*, 2004, **94**, 391–399.

15 (*a*) H. Garcia, A. S. Barros, C. Gonçalves, F. M. Gama and A. M. Gil, *Eur. Polym. J.*, 2008, **44**, 2318–2329; (*b*) J. Carvalho, C. Gonçalves, A. M. Gil and F. M. Gama, *Eur. Polym. J.*, 2007, **43**, 3050–3059; (*c*) J. M. Carvalho, M. A. Coimbra and F. M. Gama, *Eur. Polym. J.*, 2009, **75**, 322–327; (*d*) E. F. Okieimen and F. Egharevba, *Eur. Polym. J.*, 1992, **28**, 415–417; (*e*) S. Pal, T. Nasim, A. Patra, S. Ghosh and A. B. Panda, *Int. J. Biol. Macromol.*, 2010, **47**, 623–631.

16 V. Rana, P. Rai, A. K. Tiwari, R. S. Singh, J. F. Kennedy and C. J. Knill, *Carbohydr. Polym.*, 2011, **83**, 1031–1047.

17 (*a*) J. S. Belkas, C. A. Munro, M. S. Shoichet, M. Johnston and R. Midha, *Biomaterials*, 2005, **26**, 1741–1749; (*b*) O. Hossein, P. Kinam and K. U. Jose, *J. Bioact. Compat. Polym.*, 2010, **25**, 483–497; (*c*) F. M. Veronese, G. Ceriotti, G. Keller, S. Lora and M. Carenza, *Int. J. Radiat. Appl. Instrum., Part C*, 1990,

35, 88–96; (*d*) M. Carenza, S. Lora, P. Caliceti, O. Schiavon and F. M. Veronese, *Radiat. Phys. Chem.*, 1993, **42**, 897–901; (*e*) B. Tasdelen, N. K. Apohan, O. Guven and B. M. Baysal, *Radiat. Phys. Chem.*, 2005, **73**, 340–345.

18 (*a*) G. Mabilleau, M. F. Moreau, R. Filmon, M. F. Basle and D. Chappard, *Biomaterials*, 2004, **25**, 5155–5162; (*b*) B. Vazquez, M. Gurruchaga and I. Goni, *Polymer*, 1995, **36**, 2311–2314.

19 H. Omidian, S. A. Hashemi, P. G. Sammes and I. Meldrum, *Polymer*, 1998, **39**, 816–823.

20 B. Singh, N. Sharma and N. Chauhan, *Carbohydr. Polym.*, 2007, **69**, 631–643.

21 (*a*) Q. Wang, Z. Dong, Y. Du and J. F. Kennedy, *Carbohydr. Polym.*, 2007, **69**, 336–343; (*b*) K. Ganguly, T. M. Aminabhavi and A. R. Kulkarni, *Ind. Eng. Chem. Res.*, 2011, **50**, 11797–11807.

22 G. R. Bardajee, A. Pourjavadi and R. Soleyman, *Colloids Surf., A*, 2011, **392**, 16–24.

23 M. Donbrow and Y. Samuelov, *J. Pharm. Pharmacol.*, 1980, **32**, 463–470.

24 M. Gibaldi and S. Feldman, *J. Pharm. Sci.*, 1967, **56**, 1238–1242.

25 S. Kiortsis, K. Kachrimanis, T. Broussali and S. Malamataris, *Eur. J. Pharm. Biopharm.*, 2005, **59**, 73–83.

26 N. A. Peppas, *Pharm. Acta Helv.*, 1985, **60**, 110–111.

27 R. W. Korsemeyer, R. Gurny, E. Doelker, P. Buri and N. A. Peppas, *Int. J. Pharm.*, 1983, **15**, 25–35.

28 T. Higuchi, *J. Pharm. Sci.*, 1961, **50**, 874–875.

29 A. W. Hixson and J. H. Crowell, *Ind. Eng. Chem.*, 1931, **23**, 923–931.

30 M. Kopcha, N. G. Lordi and K. J. Toja, *J. Pharm. Pharmacol.*, 1991, **43**, 382–387.

31 WHO, Technical Report Series, no. 953, Annex. 2, 2009.

